EXTENDED PDF FORMAT
SPONSORED BY

BIO-RAD

http://discover.bio-rad.com



Homo erectus Calvarium from the Pleistocene of Java

Hisao Baba, *et al.*

Science **299**, 1384 (2003);
DOI: 10.1126/science.1081676

The following resources related to this article are available online at www.sciencemag.org (this information is current as of December 18, 2006):

Updated information and services, including high-resolution figures, can be found in the online version of this article at:
http://www.sciencemag.org/cgi/content/full/299/5611/1384

Supporting Online Material can be found at:
http://www.sciencemag.org/cgi/content/full/299/5611/1384/DC1

This article **cites 13 articles**, 3 of which can be accessed for free:
http://www.sciencemag.org/cgi/content/full/299/5611/1384#otherarticles

This article has been **cited by** 13 article(s) on the ISI Web of Science.

This article appears in the following **subject collections**:
Anthropology
http://www.sciencemag.org/cgi/collection/anthro

Information about obtaining **reprints** of this article or about obtaining **permission to reproduce this article** in whole or in part can be found at:
http://www.sciencemag.org/help/about/permissions.dtl

Downloaded from www.sciencemag.org on December 18, 2006

Science (print ISSN 0036-8075; online ISSN 1095-9203) is published weekly, except the last week in December, by the American Association for the Advancement of Science, 1200 New York Avenue NW, Washington, DC 20005. Copyright c 2005 by the American Association for the Advancement of Science; all rights reserved. The title SCIENCE is a registered trademark of AAAS.

ously identified. The structure identified here as the anterior skirt has been illustrated previously but identified as an anterior branchial vessel, an anterior projection, or lobated structures (*4*). Other structures, such as the heart and copulatory organ (*4*, *7*, *8*), find no counterpart in our yunnanozoan material.

Hitherto the yunnanozoan gills have been regarded as internal structures (*16*), integral to the perforated pharynx and comparable to those of the lamprey ammocoete larva (*4*). In *H. jianshanensis*, the gills formed external arches, attached to the outer surfaces of the dorsal and ventral units. An external position of the gills makes the location of any pharyngeal openings more problematic. No evidence exists for openings in the cuticle of the median zone. However, well-defined circular structures [also seen in *Y. lividum* (*7*, *8*)] adjacent to the ventral terminations of the gills, each consisting of an outer annulus and central zone (Fig. 2, A and B), could represent individual openings, each defined by a narrow rim. An alternative possibility is that these circular structures represent attachment discs for the gills.

Earlier suggestions for a phylogenetic connection to the vetulicolians, interpreted as stem-group deuterostomes (*17*), can be supported by our observations of *H. jianshanensis*. In particular, the prominent dorsal and ventral units are similar to the carapace-like anterior of *Vetulicola*, although in yunnanozoans, the intervening cuticular median zone is expanded. Provisionally, we identify the circular structures on the lower unit as pharyngeal openings, ventral to the equivalent structures in the vetulicolians. The yunnanozoans, therefore, are interpreted as a deuterostome stem group, but the possession of gills suggests that phylogenetically they are more crownward than the vetulicolians. If the dorsal and ventral nerve cords are correctly identified, this would find a counterpart in enteropneust hemichordates; in other respects, the yunnanozoan body plan is markedly divergent.

Deuterostome phylogeny is problematic, both because of the disparate nature of the extant phyla and the seemingly bizarre nature of the candidate stem taxa. Although molecular data on deuterostomes (*18*, *19*) offer new insights into previously unexpected relationships, the fossil records of groups such as calcichordates (*20*), vetulicolians (*17*), and yunnanozoans are of central importance. In particular, it is possible that the diagnostic pharyngeal arches are effectively composite structures, being derived from a pharyngeal opening that evolved [in the vetulicolians (*17*)] before the appearance of prominent gill arches. In this scenario, only subsequently did these gills migrate to an internal (and more protected) position.

Systematic Paleontology is as follows:

?Phylum Vetulicolia

Class Yunnanozoa Dzik 1995 (*5*)

Family Yunnanozoonidae Dzik 1995 (*5*)

Genus *Haikouella* Chen *et al.* 1999 (*4*)

Haikouella jianshanensis n. sp.

Etymology: Specific name refers to Jianshan (peaked hill), where the material was collected.

Holotype: ELI-0010001(226)

Other material: More than 1420 specimens.

Stratigraphy and locality: Qiongzhusi (Chiongchussu) Formation, near base of Yu'anshan Member (*Eoredlichia* Zone), Lower Cambrian. Specimens collected from Jianshan, about 2 km east of Ercai village, Haikou, near Kunming, Yunnan.

Diagnosis: Anterior of main body consisting of dorsal and ventral units, connected by membrane; six pairs of external gills, attached to both units; gills robust, bipectinate; skirtlike extension, attached to anterior end of either unit. Posterior section segmented, lightly cuticularized. Mouth large, anterior gastric cavity probably voluminous, posterior with narrow intestine.

References and Notes

1. X. Zhang, D. Shu, Y. Li, J. Han, *J. Geol. Soc. London* **158**, 211 (2001).
2. L. E. Babcock, W. Zhang, S. A. Leslie, *GSA Today* **11** (no. 2), 4 (2001).
3. X. Hou, L. Ramsköld, J. Bergström, *Zool. Scr.* **20**, 395 (1991).
4. J. Chen, D. Huang, C. Li, *Nature* **402**, 518 (1999).
5. J. Dzik, *Acta Palaeontol. Pol.* **40**, 341 (1995).
6. D. Shu, X. Zhang, L. Chen, *Nature* **380**, 428 (1996).
7. J. Chen *et al.*, *Nature* **377**, 720 (1995).
8. N. D. Holland, J. Chen, *BioEssays* **23**, 142 (2001).
9. A somewhat similar conclusion was reached by Dzik (*5*), who identified two large ventrolateral lobes in *Y. lividum*. However, he compared this structure with the sclerotic ocular rings of the conodont animal.
10. In Burgess Shale–type preservation, turbulent burial introduces sediment into spaces and cavities of the animal. Subsequent compaction greatly reduces the thickness of this sediment and converts the fossil into a series of thin films. Typically, small scarps (denoted on the interpretative drawings as hachured lines, with the hachures pointing downslope) separate the various parts of the fossil and so allow inferences on their relative position and imbrication.
11. A similar structure is identified in *Y. lividum* [figure 3B in (*7*)], where it is identified as an endostyle. A ventral aorta is identified in figure 1 of (*4*), but as a single structure.
12. The failure to recognize eyes is unlikely to be a result of taphonomic circumstances, because well-developed eyes occur in the agnathan *Haikouichthys* (*15*), as well as in a number of Chengjiang arthropods.
13. D. E. G. Briggs, A. J. Kear, *Lethaia* **26**, 275 (1994).
14. D. Shu *et al.*, *Nature* **402**, 42 (1999).
15. D. Shu *et al.*, *Nature* **421**, 526 (2003).
16. The gill bars of yunnanozoans with spaced discs are described in (*4*) and (*7*), but these are more likely to be cuticular bands, marking in *H. lanceolata* and *H. jianshanensis* the insertion points of the extended filaments and leaves, respectively.
17. D. Shu *et al.*, *Nature* **414**, 419 (2001).
18. C. B. Cameron *et al.*, *Proc. Natl. Acad. Sci. U.S.A.* **97**, 4469 (2000).
19. C. J. Winchell *et al.*, *Mol. Biol. Evol.* **19**, 762 (2002).
20. P. Dominguez, A. G. Jacobsen, R. P. S. Jefferies, *Nature* **417**, 841 (2002).

21. We thank the National Natural Science Foundation of China; the Ministry of Sciences and Technology of China; the National Geographic Society; The Royal Society; and St. John's College, Cambridge. M. Cheng, L. Guo, X. Cheng, J. Zhai, H. Guo, Y. Ji, S. Last, and A. Allen are thanked for technical assistance. M. M. Smith and an anonymous referee are thanked for constructive dialogues.

28 October 2002; accepted 15 January 2003

Homo erectus Calvarium from the Pleistocene of Java

Hisao Baba,[1,2]* Fachroel Aziz,[3] Yousuke Kaifu,[1] Gen Suwa,[4] Reiko T. Kono,[1] Teuku Jacob[5]

A *Homo erectus* calvarium [Sambungmacan 4 (Sm 4)] was recovered from Pleistocene sediments at Sambungmacan in central Java. Micro–computed tomography analysis shows a modern human–like cranial base flexion associated with a low platycephalic vault, implying that the evolution of human cranial globularity was independent of cranial base flexion. The overall morphology of Sm 4 is intermediate between that of earlier and later Javanese *Homo erectus*; apparent morphological specializations are more strongly expressed in the latter. This supports the hypothesis that later Pleistocene Javanese populations were substantially isolated and made minimal contributions to the ancestry of modern humans.

Javanese *Homo erectus* is best represented by the Early and Middle/Late Pleistocene remains found at Trinil, Sangiran, and Ngandong (*1*–*4*). Shared features of these hominids have led to the notion of continuous regional evolution in Java (*5*–*7*) as part of a broader *H. erectus* species distribution (*8*, *9*). However, the actual evolution of Asian *H. erectus* is uncertain (*7*, *8*), and phyletic relationships concerning *H. erectus*, other archaic *Homo*, and modern humans remain unresolved (*6*–*11*). Aside from the widely acknowledged increase of cerebral mass (*12*), the underlying morphogenetic basis of the transition from *H. erectus* to *H. sapiens* has only begun to be explored. Here we describe a new calvarium, Sambungmacan 4 (Sm 4). We analyzed Sm 4 by micro–computed tomography (micro-CT)–based visualization and compared it with other Javanese crania.

Downloaded from www.sciencemag.org on December 18, 2006

In the Sambungmacan area, two partial calvaria (Sm 1 and Sm 3) and a tibia fragment (Sm 2) of *H. erectus* were previously recovered (*13*–*15*). Affinities with the Ngandong series were suggested for the two calvaria (*13*, *15*), although some regarded Sm 1 as intermediate between the Trinil/Sangiran and Ngandong hominids (*6*). The new adult calvarium, Sm 4, was discovered on 1 October 2001, between Mlale village of the Jenar district and Cemeng village of the Sambungmacan district in central Java (Fig. 1). It was found 4 km west of where Sm 1 was found in 1973, and 100 m upstream from where Sm 3 was discovered in 1997 (*15*). The specimen was found along the Solo River during the collection of sand for construction material, but it shows no obvious signs of fluvial transport or surface weathering. Fossiliferous sediments of Middle Pleistocene age crop out upstream (*16*). Sm 4 preserves all calvarial elements, including those of the cranial base except the ethmoid. There is no obvious postmortem distortion, and osseous surface detail is excellent.

Sm 4 is larger than most other *H. erectus* specimens and probably belonged to a male. Most cranial sutures show minimal to moderate closure, suggesting that the individual was mid-

[1]Department of Anthropology, National Science Museum, Hyakunincho, Shinjuku-ku, Tokyo 169-0073, Japan. [2]Department of Biological Science, The University of Tokyo, Hongo, Bunkyo-ku, Tokyo 113-0033, Japan. [3]Laboratory of Vertebrate Paleontology, Geological Research and Development Centre, Jl. Diponegoro 57, Bandung 40122, Indonesia. [4]The University Museum, The University of Tokyo, Hongo, Bunkyo-ku, Tokyo 113-0033, Japan. [5]Laboratory of Bio- and Palaeoanthropology, Gadjah Mada University, Yogyakarta 55002, Indonesia.

*To whom correspondence should be addressed. E-mail: baba@kahaku.go.jp

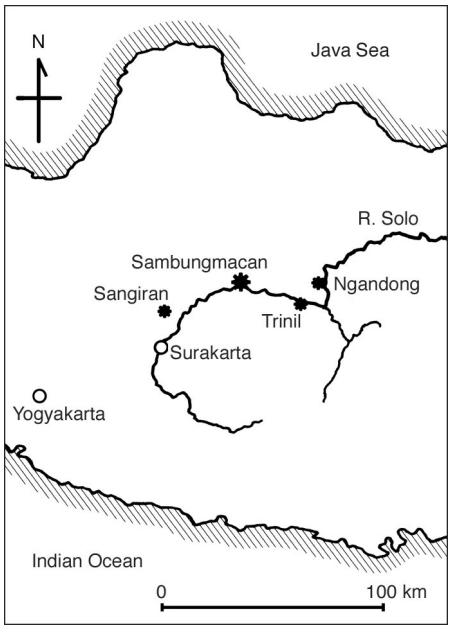


Fig. 1. Location map.

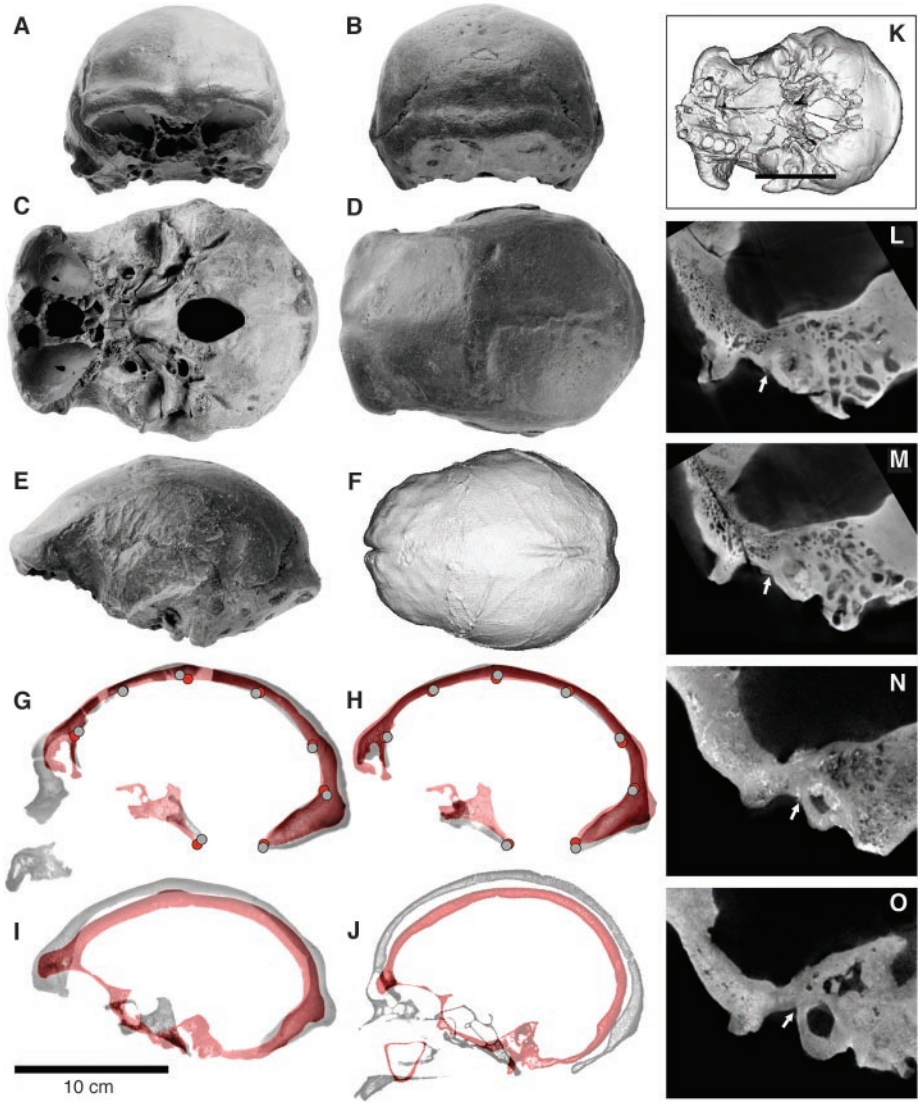


Fig. 2. Views of Sm 4 and CT imagery of Sm 4 and comparative materials. Anterior (**A**), posterior (**B**), basal (**C**), superior (**D**), and lateral (**E**) views of Sm 4 are shown. (**F**) Superior view of virtual endocast. Superimposed midsagittal sections of Sm 4 (red) and Sangiran 17 (gray) (**G**) and of Sm 4 (red) and Ngandong 12 (gray) (**H**) are shown. (**I**) Mid- (gray) and parasagittal (red) sections of Sm 4 and (**J**) of a modern human cranium. Sagittal micro-CT sections of the mandibular fossa were taken just medial to the lateral edge of the tympanic, which position is shown for Sangiran 17 (**K**). The sections are Sangiran 17 right (**L**) and left (**M**), Sm 4 left (**N**), and Ngandong 12 left (**O**). Arrows indicate the position of the squamotympanic fissure. Landmarks plotted in (G) and (H) were determined from the serial micro-CT images as follows: anterior pole of the endocranium, midpoint on the internal endocranial contour between the anterior pole point and internal bregma, internal bregma, midpoint on the internal endocranial contour between the internal bregma and lambda, internal lambda, posterior pole of the endocranium, opisthion, and basion. The anterior and posterior pole points were defined as the most anterior and posterior points in an axis parallel to the glabella-inion line, in the serial parasagittal sections, projected onto the midsagittal section. Registration of Sm 4 and Sangiran 17 or Ngandong 12 was done by the Procrustes technique of superimposition (centroid size standardization and least-squares fit of the eight landmarks). Parasagittal sections of (I) and (J) were taken through the maximum anterior projections of the temporal pole of the middle cranial fossa. Images (L) to (O) were obtained by reformatting the serial micro-CT images. In Ngandong 12 (O), the entire squamous portion of the fossa inclines posterosuperiorly, so that the deepest part of the fossa occurs posteriorly at the squamotympanic fissure. Contrary to previous assessments (*7*, *15*), Sangiran 17 does not show this peculiar morphology. The squamous portion of the fossa exhibits a broad and deep concavity placed anterior to the squamotympanic fissure. This is typical of both modern humans and other fossil hominids. The micro-CT image (M) reveals a postmortem crack passing through the deepest portion of the left mandibular fossa of Sangiran 17. Sm 4 is intermediate between Ngandong 12 and Sangiran 17.

Downloaded from www.sciencemag.org on December 18, 2006

Table 1. Cranial base metrics of Sm 4 and the comparative materials. Cranial base angle 1 (CBA1) is the angle between the basion-sella and sella–foramen caecum and CBA4 is the angle between the clival plane and planum sphenoideum (*34*). TP1 is the ratio between the sella–temporal pole distance and the sella–foramen caecum length. The temporal pole point is defined as the most anterior point of the middle cranial fossa projected onto the midsagittal plane perpendicular to the sella–foramen caecum line. ORA1 is the angle between the sella–foramen caecum line and the line connecting the posterosuperior point of the tuberculum sellae and the anteroinferior pole of the anterior cranial fossa projected onto the midsagittal section. The anteroinferior pole point was defined on the parasagittal section passing through the middle of the foramen ovale. Values derived from the right and left sides were averaged in both TP1 and ORA1. The TP1 estimate of Ngandong 12 is based on its temporal pole position and preserved sella turcica floor. The approximate locations of the sella and foramen caecum were derived from Procrustes superimposition of Ngandong 12 with Sm 4.

		Cranial base angle						Temporal pole position			Orbital roof angle		
		CBA1			CBA4			TP1			ORA1		
		Mean	SD	Range	Mean	SD	Range	Mean	SD	Range	Mean	SD	Range
Modern human	This study, $n = 9$	136	4.7	128.5–141	110	8.5	98–122	0.40	0.046	0.35–0.50	11.9	3.58	6–18
	Spoor 1997 (*35*), $n = 48$	138	4.9		–			–			–		
	McCarthy 2001 (*34*), $n = 60$	136	5.2		111	6.8		–			–		
	Ross and Henneberg 1995 (*22*), $n = 93$	–			112	7.4	92–135	–			–		
Sm 4	This study	141			97			0.30			20		
Ngandong 12	This study	–			–			(0.29)			–		
OH 9	Ross and Henneberg 1995 (*22*)	–			93–104			–			–		

Table 2. Cranial characters that differentiate the Javanese *H. erectus* subgroups, and the phenetic condition of the Sambungmacan calvaria (*19*). These characters were taken or modified from the literature (*5*, *7*, *8*, *13*, *15*, *17*), except for item 11. For items 2 through 22, the morphological condition of interest is listed in the first column. Each subgroup/specimen exhibits either the listed condition "+," a different condition "–," or a partial expression of that condition "int." Parentheses indicate notably variable conditions. Item 14 refers to a mandibular fossa characterized not only by an anteroposteriorly short, deep fossa with the squamotympanic fissure situated in the deepest portion, but also by a laterally extended tympanic plate forming the "posterior wall" of the fossa and minimal or no development of the postglenoid process (Fig. 2). The African *H. erectus* OH 9 differs in the latter aspects. Characters 7 to 10, 14, 16, 18, and 20 to 22 are possibly uniquely derived features characteristic of the Ngandong series.

Cranial characters	Trinil/Sangiran	Sm 1	Sm 3	Sm 4	Ngandong
1. Cranial capacity (cm^3)	813–1059	1035	918	1006	1013–1251
2. Relatively high vault	(–)	+	+	–	(+)
3. Moderately swollen frontal squama and posterior parietals	–	+	+	int	+
4. Postorbital constriction comparatively weaker	–	+	+	+	+
5. Strong temporal gutter	–	int	–	+	+
6. Reduced relative area of temporal muscle attachment	–	+	+	+	+
7. Extremely linear supraorbital torus in front view	–	+?	+	int	(+)
8. Laterally thickened supraorbital torus	–	int	+	+	+
9. No supraglabellar depression with right and left supratoral planes discontinuous	–	int	+	int	(+)
10. Extensive, plateau-like angular torus	(–)	+	+?	+	(+)
11. Antero-posteriorly elongated parietal incisura	–	int	+	int	+
12. Wide supramastoid sulcus	–	int	+	int	(+)
13. Large mastoid with triangular base	–	int	+	int	+
14. Specialized mandibular fossa morphology	–	int	+	int	+
15. Well-developed tympano-mastoid fissure	(–)	int	+	+	+
16. Less extensive digastric fossa associated with well-developed paramastoid crest	–	int	?	int	+
17. Vertically set occipital squama	–	+	+	+	+
18. Marked projection of occipital torus	(–)	–	–	+	(+)
19. Lower arm of occipital torus stronger than the upper	–	int	+	int	(+)
20. Extreme expression of an excavated nuchal planum	–	–	–	–	(+)
21. Opisthionic recess of foramen magnum present	–	?	+	+	+
22. Strong postcondyloid tuberosity	–	?	+	+	+

dle-aged or younger. There are several shallow depressions on the intact frontal squama and anterior parietals, the surfaces of which show characteristics of healed scars, as has been reported for several calvaria from Ngandong (*17*), 40 km east of Sambungmacan.

The overall morphology of Sm 4 is that of *H. erectus*, and it shares many features with Javanese representatives of the species (Fig. 2, A to E). The vault is long and low, with the maximum breadth across the supramastoid crests. The thick supraorbital torus is relatively straight in front view, as is typical in *H. erectus* of Java. The strong coronal and parietal keels are continuous with the weaker frontal keel via the bregmatic eminence. The occipital bone is sharply angled at the well-developed occipital torus. Suprameatal and supramastoid crests are marked, and angular tori are extensive on the mastoid angles of the parietals. The thick tympanic plates are coronally oriented. The styloid process is lacking. Sm 4 lacks characteristic features of Chinese *H. erectus* represented by the Zhoukoudian specimens, such as the continuous supratoral sulcus, steeply rising frontal squama with salient tuberosities, narrow occiput, relatively large biauricular breadths with markedly inclined temporal walls, and medially restricted petrosal crest (*5*, *7*, *17*, *18*).

The endocranial capacity of Sm 4 is 1006 cm^3, on the basis of volume rendering of 592 serial CT scans taken at a slice thickness and pitch of 340 μm (*19*). The virtual endocast (Fig. 2F) exhibits left occipital petalia, as is common in other *H. erectus* remains and modern humans (*12*). The internal occipital crest is broad, and inion is widely separated from endinion. The frontal sinus is restricted relative to Euro-African specimens such as Kabwe and Petralona (*20*), with limited lateral and no posterior extensions.

Presumed male representatives of the Sangiran and Ngandong series, Sangiran 17 and Ngandong 12, that best preserve the cranial base were compared with Sm 4. In sagittal profile, the endocranial contour is comparably platycephalic in all three crania, but Ngandong 12 exhibits a slightly more depressed cranial base and higher frontal profile than does Sm 4

Downloaded from www.sciencemag.org on December 18, 2006

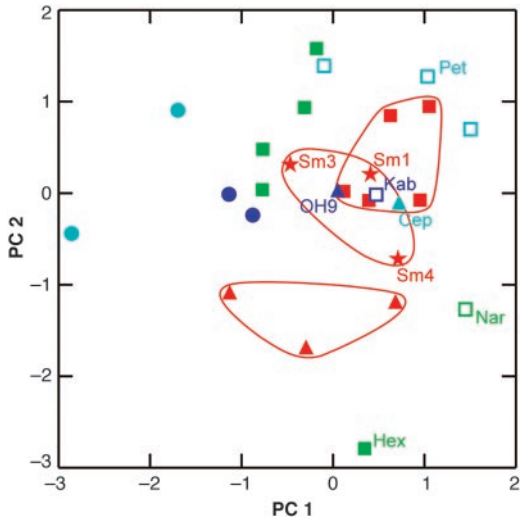


Fig. 3. First and second principal component (PC) scores of linear measurements of the whole vault (see fig. S1 for results on the individual bones). Variables are as follows: maximum cranial length, minimum frontal breadth, maximum cranial breadth, biasterionic breadth, and porion-bregma height. PC 1 (which accounts for 76% of the variance) gives greater scores if the vault is larger overall; PC 2 (which accounts for 11% of the variance) gives greater scores if the biasterionic breadth is narrower and the vault is higher. *H. erectus* (solid symbols) and later archaic *Homo* (open symbols) specimens dated between 1.8 to 1.4 million years (circles), 1.4 to 0.7 million years (triangles), and 0.7 million years and younger (squares) from Indonesia (red), Africa (blue), East Eurasia (green), and West Eurasia (sky blue) are included. The Sambungmacan specimens are indicated by stars. Hex, Hexian; Nar, Narmada; Kab, Kabwe; Cep, Ceprano; Pet, Petralona. Symbols without specimen names are as follows: red triangles, Trinil/Sangiran; red squares, Ngandong; green squares, Zhoukoudian; blue circles, East Turkana; sky blue circles, Dmanisi; sky blue squares, Sima de los Huesos.

or Sangiran 17 (Fig. 2, G and H). The thickness of the frontal bone at the glabella or nasion is weaker in Sm 4 and Ngandong 12 than in Sangiran 17. Overall, differences in cranial morphology tend to be more clearly manifested externally, whereas all three crania revealed a remarkably similar endocranial shape.

The cranial base flexion of *H. erectus* has hitherto been estimated in a single damaged specimen, OH 9, from the early Pleistocene of Africa. Our results show that the cranial base flexion of Sm 4 was as strong as in modern humans (Table 1 and Fig. 2, I and J) (*21*), as was suggested by OH 9 (*22*), but reports of two Kenyan specimens from the earliest Pleistocene have left open the possibility that early *H. erectus* might have been characterized by a less flexed condition (*23*). The strong cranial base flexion of Javanese *H. erectus* suggests that midsagittal flexion did not play a decisive role in either the reduction of facial projection or the emergence of neurocranial globularity [compare with (*24*, *25*)].

Despite the derived condition of the midsagittal endocranial base, the structure of the more lateral endocranial base of Javanese *H. erectus* is distinct from that of modern humans (Fig. 2, I and J). The orbital axis of *Australopithecus* and, to a lesser degree, archaic *Homo* has been described as more anterodorsally oriented than in modern humans (*20*, *22*). Although the same axis could not be measured in Sm 4, the inclination of the superior orbital roof is more anterodorsal than in modern humans (Table 1). In Sm 4 and Ngandong 12, the middle cranial fossa does not extend anteriorly as far as in modern humans (*26*) (Table 1). Changes in orbital orientation and temporal pole position are likely correlates of a general restructuring of anterior and middle cranial fossae associated with cerebral expansion. The length between the sella and the anterior temporal pole in our CT data sets corresponds to the "anterior sphenoid length" of previous radiographic studies (*24*). Our results indicate that the primitive condition of *Homo* was probably a shorter sphenoid, in concert with Spoor *et al.*'s (*27*) analysis of archaic *Homo*. The importance of the lateral cranial base in the development of facial form has been emphasized in modern humans (*28*), although such structural and developmental relations remain unclarified in evolutionary perspective.

The midsagittal cranial base flexion of archaic *H. sapiens* such as Kabwe has been suggested to be weaker than in modern humans by about 15° (*22*, *24*, *25*). The apparent contradiction of stronger cranial base flexion in Javanese *H. erectus* may reflect any of the following possibilities. First, it may simply reflect normal levels of intraspecific variation, with both *H. erectus* and archaic *H. sapiens* possessing comparable modal conditions. An inferred strong flexion in Bodo (*29*), another African example of archaic *H. sapiens*, supports this hypothesis. Second, a strong cranial base flexion might have been characteristic only of later *H. erectus* but not of *H. erectus* in general, a hypothesis contradicted by the OH 9 estimate. Finally, archaic *H. sapiens* may have secondarily acquired a more extended cranial base from the ancestral *H. erectus* condition. A possible mechanism for this might be a situation in which a slightly greater degree of postnatal extension of the cranial base occurred through interrelation with somatic growth.

Our analyses also offer new insights into the evolutionary history of Javanese *H. erectus* and into the ongoing controversy surrounding the origin of modern humans. Sm 4 is similar to Sangiran 17 and other Trinil/Sangiran specimens in its platycephalic cranial shape and lack of a strongly excavated nuchal plane. Sm 4 and Sm 1 are intermediate between Trinil/Sangiran and Ngandong, or close to Ngandong, in many other features (Table 2). Sm 4 also exhibits the rare presence of a foramen ovale subdivided by a bony bridge, as do some of the Ngandong specimens (*17*). In most of these features, Sm 3 exhibits the Ngandong series condition (*15*) (Table 2).

We conducted principal component analyses (PCAs) of several sets of metric data (*19*) to examine phenetic similarities among specimens without making a priori assumptions about grouping. A recent overview of Asian *H. erectus* contrasted the Javanese and Chinese samples from PCAs of cranial capacity and four cranial vault measurements (*7*, *30*). Our results of five length, breadth, and height variables of the cranial vault (Fig. 3) and evaluations of individual bones (fig. S1) demonstrate the intermediate state of the Sambungmacan specimens within the Javanese series in relative cranial height and in temporal bone size and shape. In parietal and occipital bone size and shape, the Javanese crania cluster tightly, with subsample ranges of variation overlapping extensively.

The combined evidence suggests that Sm 4 (and Sm 1) represent a transition linking the Trinil/Sangiran and Ngandong hominids morphologically and possibly temporally. Our analysis also demonstrates that later Javanese *H. erectus* exhibits a suite of unique features (Table 2). These include aspects of mandibular fossa and foramen magnum morphologies (*15*, *17*), which changed from an ancestral condition (the Trinil/Sangiran condition, which is closer to that seen in modern humans), to one more derived in later Javanese forms (Ngandong) (Fig. 2, L to O). The morphological distinctiveness of the Javanese *H. erectus* lineage apparently intensified over time. This might have occurred through episodic range contraction and fragmentation, as glacial cycles recurred throughout the Pleistocene (*7*, *31*). If *H. erectus* avoided tropical forest habitats, gene pool fragmentation was probably accentuated in peak interglacial periods, although details of the regional paleoenvironmental history and habitat preference of *H. erectus* are little known (*32*, *33*).

References and Notes

1. R. Larick *et al.*, *Proc. Natl. Acad. Sci. U.S.A.* **98**, 4866 (2001).
2. M. Hyodo *et al.*, *J. Hum. Evol.* **43**, 27 (2002).
3. G. D. Van den Bergh, J. De Vos, P. Y. Sondaar, F. Aziz, *Indo-Pac. Prehist. Assoc. Bull.* **14**, 7 (1996).
4. C. C. Swisher III *et al.*, *Science* **274**, 1870 (1996).
5. A. P. Santa Luca, *The Ngandong Fossil Hominids: A Comparative Study of a Far Eastern Homo erectus Group* (Department of Anthropology, Yale Univ., New Haven, CT, 1980).
6. M. H. Wolpoff, *Paleoanthropology* (McGraw-Hill, New York, ed. 2, 1999).
7. S. C. Antón, *Am. J. Phys. Anthropol.* **118**, 301 (2002).
8. G. P. Rightmire, *The Evolution of Homo erectus: Comparative Anatomical Studies of an Extinct Human Species* (Cambridge Univ. Press, Cambridge, 1990).

Downloaded from www.sciencemag.org on December 18, 2006

9. B. Asfaw *et al.*, *Nature* **416**, 317 (2002).
10. J. Hawks *et al.*, *J. Hum. Evol.* **39**, 1 (2000).
11. C. Stringer, *Philos. Trans. R. Soc. London Ser. B* **357**, 563 (2002).
12. R. L. Holloway, in *Handbook of Human Symbolic Evolution*, A. Lock, C. R. Peters, Eds. (Blackwell, Oxford, 1999), pp. 74–125.
13. T. Jacob, in *Homo erectus: Papers in Honor of Davidson Black*, B. A. Sigmon, J. S. Cybulski, Eds. (Univ. of Toronto Press, Toronto, Canada, 1981), pp. 87–104.
14. S. Matsu'ura *et al.*, *Curr. Anthropol.* **41**, 297 (2000).
15. E. Delson *et al.*, *Anat. Rec.* **262**, 380 (2001).
16. Vertebrate fossils recovered from the Sm 4 findspot vary in preservation, suggesting a mixed assemblage composed of fossils from multiple sources upstream. Outcrops that we identified, within 6 km upstream of the find, include those that belong to the traditional Kabuh Formation of this area. On the basis of its adhering matrix, Sm 4 is likely to have derived from this series.
17. F. Weidenreich, *Anthropol. Pap. Am. Mus. Nat. Hist.* **43**, 205 (1951).
18. F. Weidenreich, *Palaeontol. Sin. New Ser. D* **10**, 1 (1943).
19. Materials and methods are available as supporting material on *Science* Online.
20. H. Seidler *et al.*, *J. Hum. Evol.* **33**, 691 (1997).
21. Our micro-CT analysis of Ngandong 12 revealed a damaged clivus and missing dorsum sellae, tuberculum sellae, and planum sphenoideum regions. This precludes a numerical evaluation of its cranial base flexion. The entire region from the sella turcica to the planum sphenoideum is missing in Sangiran 17. However, the floor of the sella turcica is preserved in Ngandong 12, and the clivus in Sangiran 17, allowing a comparison of approximate alignments with Sm 4 (Fig. 2, G and H). This suggests a cranial base, in both Ngandong 12 and Sangiran 17, that is broadly compatible with the Sm 4 condition of flexion. As far as we are aware, no account of cranial base flexion of Ngandong 7 has been published.
22. C. Ross, M. Henneberg, *Am. J. Phys. Anthropol.* **98**, 575 (1995).
23. F. Spoor, *Am. J. Phys. Anthropol. Suppl.* **30**, 288 (2000).
24. D. E. Lieberman, C. F. Ross, M. J. Ravosa, *Yrbk. Phys. Anthropol.* **43**, 117 (2000).
25. D. E. Lieberman, B. M. McBratney, G. Krovitz, *Proc. Natl. Acad. Sci. U.S.A.* **99**, 1134 (2002).
26. In Sm 4, the anterior temporal pole outline intersects the midline cranial base profile close to the tuberculum sellae, whereas the same intersection in modern humans occurs at a position approximately at the middle of the planum sphenoideum (Fig. 2, I and J).
27. F. Spoor, P. O'Higgins, C. Dean, D. E. Lieberman, *Nature* **397**, 572 (1999).
28. M. Bhat, D. E. Enlow, *Angle Orthodont.* **55**, 269 (1985).
29. F. Bookstein *et al.*, *Anat. Rec.* **257**, 217 (1999).
30. S. Antón, S. Marquez, K. Mowbray, *J. Hum. Evol.* **43**, 555 (2002).
31. G. Hewitt, *Nature* **405**, 907 (2000).
32. G. D. van den Bergh, J. de Vos, P. Y. Sondaar, *Palaeogeogr. Palaeoclimatol. Palaeoecol.* **171**, 385 (2001).
33. F. J. Gathorne-Hardy, Syaukani, R. G. Davies, P. Eggleton, D. T. Jones, *Biol. J. Linn. Soc.* **75**, 453 (2002).
34. R. C. McCarthy, *J. Hum. Evol.* **40**, 41 (2001).
35. F. Spoor, *S. Afr. J. Sci.* **93**, 182 (1997).

36. We thank Darsono for the recovery of Sm 4; Sudijono, T. Sihombing, I. Kurniawan, A. Hikmat, E. Indriati, A. Suprijo, P. H. Sulistyarto, R. A. Suriyanto, J. M. Susanto, and people of Mlale and Cemeng for fieldwork; J. Arif for access to Tjg-1993.05; H. Otsuka for stratigraphic interpretations; T. Suzuki for observations of possible traumatic bone alteration on Sm 4; F. Spoor for comments on *H. erectus* cranial base lengths and flexion; S. Matsukawa and M. Chubachi for assistance; and T. White and E. Delson for suggestions. We thank the Geological Research and Development Centre, Bandung, for permission and support. This work was supported by the National Science Museum, Tokyo, and the Japan Society for the Promotion of Science.

Supporting Online Material
www.sciencemag.org/cgi/content/full/299/5611/1384/DC1
Materials and Methods
Fig. S1
Tables S1 and S2

19 December 2002; accepted 27 January 2003

Foraging Adaptation and the Relationship Between Food-Web Complexity and Stability

Michio Kondoh

Ecological theory suggests that complex food webs should not persist because of their inherent instability. "Real" ecosystems often support a large number of interacting species. A mathematical model shows that fluctuating short-term selection on trophic links, arising from a consumer's adaptive food choice, is a key to the long-term stability of complex communities. Without adaptive foragers, food-web complexity destabilizes community composition; whereas in their presence, complexity may enhance community persistence through facilitation of dynamical food-web reconstruction that buffers environmental fluctuations. The model predicts a linkage pattern consistent with field observations.

Ecological theory (*1*–*5*) suggests that complexity (high species richness, dense trophic links) destabilizes food webs. "Real" ecosystems often support large numbers of species interacting in highly complex networks of direct and indirect pathways (*6*–*9*). To resolve this apparent paradox, several hypotheses have been proposed, including ones attributing "real" food-web stability to dominance of stabilizing food-web architecture (*10*, *11*). These studies have considered relatively static topological food-web features such as distribution of interaction strength (*10*) and trophic links (*11*). I propose that "flexibility" in food-web structure, arising from the consumers' adaptive behavioral (*12*, *13*) or evolutionary (*14*, *15*) switches in food choice in response to qualitative and quantitative resource changes, stabilizes complex food webs.

Adaptation is critical to food-web dynamics (*16*) and influences food-web stability (*17*). This study considers food-web models having more realistic and wide-ranging complexity, where the degree of flexibility is manipulated by systematically changing both the fraction of adaptive foragers and their adaptation rate. This provides a comprehensive picture of the synergistic effects of food-web complexity and adaptation on food-web stability.

Consider a food web comprising N species, any pair of which are connected to each other with probability C (≤ 1; connectance). In determining trophic link direction, I used two models, random (*18*) and cascade (*4*, *18*), which generate different substructures (*19*). Suppose that consumers cannot consume different resource species simultaneously because of the prey's patchy distribution (*12*), the capturing strategy for different prey (*12*), or the consumer's sensory and cognitive constraints for discriminating between prey (*20*). Consumers allocate their foraging effort among possible resources and, given a fixed total foraging effort (measured by energy or time), per capita consumption rate would increase with increasing foraging efficiency and increased foraging effort allocated to the resource (*21*).

The dynamics of species i ($1 \ldots N$) biomass, X_i, is described by:

$$\frac{dX_i}{dt} = X_i\left(r_i - s_i X_i + \sum_{j \in resources} e_{ij} f_{ij} a_{ij} X_j - \sum_{j \in consumers} f_{ji} a_{ji} X_j \right) \quad (1)$$

where r_i is an intrinsic reproductive rate; s_i a self-regulation intensity; f_{ij} the foraging efficiency of species i on resource species j, defined as a per capita foraging rate when all foraging efforts are allocated to resource j; a_{ij} the foraging effort of species i allocated to resource j ($\sum_{j \in resources} a_{ij} = const. = 1$, and $a_{ij} = 0$ when species i does not feed on species j); and e_{ij} the metabolic rate of species i consuming species j. Hereafter, e_{ij} is, for simplicity, set to a biologically feasible (*22*, *23*) constant value, e (here $e = 0.15$, but for $e = 0.01$ to 0.35 the value does not alter the main result).

I used community persistence, the probability that all species persist for a given time in fluctuating environments, as an index of food-web stability. As biological parameters change over space and time by environmental disturbances, the community persisting in the wider parameter region is more likely to be observed in nature (*3*). To estimate the effects of complexity on community persistence, I calculated the probability of community persistence in an ensemble of stochastically gen-

Center for Ecological Research, Kyoto University, Kamitanakami, Otsu 520-2113, Japan.

Present address: Cardiff School of Biosciences, Cardiff University, Post Office Box 915, Cardiff CF10 3TL, UK. E-mail: kondohm@cf.ac.uk

Downloaded from www.sciencemag.org on December 18, 2006